

Micka Ullman

THE EARLY PRE-POTTERY  
NEOLITHIC B SITE  
AT NESHER-RAMLAL QUARRY  
(NRQN), ISRAEL



THE ZINMAN INSTITUTE OF ARCHAEOLOGY  
UNIVERSITY OF HAIFA



Bouky B. Management  
Projects & Promotions LTD

THE EARLY PRE-POTTERY NEOLITHIC B SITE  
AT NESHER-RAMLAL QUARRY (NRQN), ISRAEL



MICKA ULLMAN

THE EARLY PRE-POTTERY  
NEOLITHIC B SITE  
AT NESHER-RAMLAL QUARRY  
(NRQN), ISRAEL

With contributions by Amos Frumkin, Michael B. Toffolo, Elisabetta Boaretto,  
Lena Brailovsky, Julia Abramov, Roni Zuckerman-Cooper, Lior Weissbrod,  
Heeli C. Schechter, Daniella E. Bar-Yosef Mayer, Valentina Caracuta and Steve Weiner

*Scientific editor*  
**Reuven Yeshurun**

המכון לארכיאולוגיה ע"ש זינמן, אוניברסיטת חיפה  
THE ZINMAN INSTITUTE OF ARCHAEOLOGY, UNIVERSITY OF HAIFA



בוקי ב. מנג'מנט  
Projects & Promotions Ltd



The Zinman Institute of Archaeology: <http://arch.haifa.ac.il>

*Project management:* Bouky B. Management Projects & Promotions Ltd.

*Maps, plans, and cross-sections:* Viatcheslav Pirsky and Sergey Alon

*Photographs:* Anya Hayat and Tomer Appelbaum

*Language editor:* Miriam Feinberg Vamosh

*Drawings:* Sergey Alon

*Design and layout:* Anya Hayat

Font Cover : Helwan points (photographer: Anya Hayat)

Back Cover: Aerial photo of the Neshet-Ramla quarry area (photographer: Tal Rogovsky)

ISBN: 978-965-7547-08-3

© 2020 The Zinman Institute of Archaeology, University of Haifa

Printed by: Printiv, Jerusalem 2020

*Dedicated to my grandparents  
Yehuda and Simcha Avrahami*



# CONTENTS

PREFACE .....	IX
LIST OF AUTHORS .....	XI
LIST OF FIGURES, TABLES AND PLATES .....	XII
CHAPTER 1: INTRODUCTION .....	1
<i>Micka Ullman</i>	
CHAPTER 2: GEOLOGY OF AN EARLY HOLOCENE SINKHOLE (NRQN), ISRAEL.....	9
<i>Amos Frumkin and Micka Ullman</i>	
CHAPTER 3: STRATIGRAPHY AND MANMADE FEATURES .....	17
<i>Micka Ullman</i>	
CHAPTER 4: RADIOCARBON DATING .....	33
<i>Michael B. Toffolo and Elisabetta Boaretto</i>	
CHAPTER 5: THE FLINT ASSEMBLAGE .....	37
<i>Micka Ullman and Lena Brailovsky</i>	
CHAPTER 6: THE GROUNDSTONE ASSEMBLAGE .....	75
<i>Micka Ullman</i>	
CHAPTER 7: SMALL FINDS .....	113
<i>Micka Ullman</i>	
CHAPTER 8: HUMAN REMAINS .....	117
<i>Julia Abramov</i>	
CHAPTER 9: THE FAUNAL ASSEMBLAGE AND WORKED BONES .....	121
<i>Roni Zuckerman-Cooper</i>	
CHAPTER 10: MICROVERTEBRATE REMAINS IN A NEOLITHIC NATURAL PITFALL TRAP ....	137
<i>Lior Weissbrod</i>	
CHAPTER 11: SHELLS AND SHELL BEADS .....	149
<i>Heeli C. Schechter and Daniella E. Bar-Yosef Mayer</i>	
CHAPTER 12: BOTANICAL REMAINS .....	169
<i>Valentina Caracuta</i>	
CHAPTER 13: SEDIMENTOLOGY AND MICROMORPHOLOGY .....	177
<i>Michael B. Toffolo and Steve Weiner</i>	
CHAPTER 14: DISCUSSION .....	193
<i>Micka Ullman</i>	
APPENDIX I: LOCI LIST .....	205





## P R E F A C E

The Pre-Pottery Neolithic B site of Neshet-Ramla (hence forth NRQN — Neshet-Ramla Quarry Neolithic) is a small filled sinkhole that was excavated by the author from September 2015 to May 2016. The site is situated within the greater el-Khirbeh archaeological site, which has been excavated since 1996 as a salvage project deriving from the ongoing work at the Neshet-Ramla quarry operated by the Neshet Israel Cement Enterprises Ltd, which has sponsored the project from its beginning until the present.

Exploration of the site started during the 1990s by the Archaeological Institute of the Hebrew University of Jerusalem. It was subsequently continued by the Israel Antiquities Authority (IAA), and since 2006 the excavations have been directed by the University of Haifa. The large-scale excavations at the site have been directed by Shlomo Kol-Ya'kov on behalf of the Zinman Institute of Archaeology at the University of Haifa. Results of the excavations have been continuously published, pertaining mainly to the Chalcolithic and Roman-Byzantine periods (see Chapter 1). The present volume focuses exclusively on the Pre-Pottery B Neolithic site.

The main author of this volume, Micka Ullman, had the honor of taking part in the excavations from 2015 until 2016, under the supervision of excavation director Shlomo Kol-Ya'kov and field director Vladimir Wolff Avrutis. Ullman led the excavations of the NRQN site and its publication, presented in this volume.

I wish to thank Shlomo Kol-Ya'kov and Vladimir Wolff Avrutis for their kind permission

to work on and publish the NRQN site and its finds. Many thanks are due to the excavation team — Salim, Wahid, Said, Mustafa, Abu Ali, Mumtaz and Mhamad from Kfar Manda as well as to Asaph Levy of the Hebrew University who worked tirelessly under harsh winter conditions and made fieldwork possible. Thanks to Viatcheslav Pirskey and Sergey Alon for producing field measurements, 3D documentation, plans and sections of the site during the excavation, and for processing the graphics for this publication. Thanks go also to Tomer Appelbaum for field photography and to Anya Hayat and Tal Rogovsky for studio photography of the various finds. Thanks to Ortal Harush, from the Computational Archaeology Laboratory of the Hebrew University's Institute of Archaeology, for 3D scanning of some of the finds. I am grateful to Yuli Gekht for designing, programing and maintaining the excavation's computerised database, which made data management fluent and efficient. Thanks to Gadi Herzlinger for his assistance in conducting statistical analysis and operating the JMP software, to Noa Klein for her help in preparing some of the graphics and assistance in operating the Illustrator software, and to Oz Varoner, of the Neshet-Ramla excavation team, for his advice and knowledge regarding prehistoric research and raw material spatial distribution of the Neshet-Ramla area.

The author is grateful to Dr. Reuven Yeshurun for his work as scientific editor of this volume and for his patient support and helpful advice during the process, to Miriam Feinberg Vamosh,

the language editor, for her pleasant approach and persistent work, and to Anya Hayat the graphic editor of this volume. My appreciation goes to the numerous scholars who shared their knowledge and advice: Prof. Nigel Goring-Morris, Prof. Erella Hovers, Prof. Na'ama Goren-Inbar, Dr. Yossi Zaidner and Dr. Uri Davidovich of the Institute of Archaeology at the Hebrew University; Prof. Ruth Shahack-Gross of the Department of Maritime Civilizations, the University of Haifa, and Prof. Danny Rosenberg of the Laboratory for Ground Stone Tools Research at the Zinman Institute of Archaeology, University of Haifa;

Prof. Yuval Goren of Ben-Gurion University of the Negev.

Special thanks are due to Bouky Boaz, the logistic manager and administrator of the project. I am grateful to the Zinman Institute of Archaeology at the University of Haifa for the academic patronage. Thanks are due to the Neshet Israel Cement Enterprises Ltd for financing this long-term project and providing plenty of technical assistance in the field. Thanks in particular to Yoram Golan, the Neshet-Ramla quarry planning and development manager.



The excavation team

## LIST OF AUTHORS

**Julia Abramov**

Dan David Center for Human Evolution and Biohistory, The Steinhardt Museum of Natural History and National Research Center, Tel Aviv University, Tel Aviv 6997801, Israel.  
julia.abramov@gmail.com

**Dr. Daniella E. Bar-Yosef Mayer**

The Steinhardt Museum of Natural History, Tel Aviv University, Tel Aviv 69978, Israel.  
baryosef@tauex.tau.ac.il

**Prof. Elisabetta Boaretto**

D-REAMS Radiocarbon Dating Laboratory, Scientific Archaeology Unit, Weizmann Institute of Science, 234 Herzl Street, Rehovot 7610001, Israel.  
elisabetta.boaretto@weizmann.ac.il

**Lena Brailovsky**

Israel Antiquities Authority, Rockefeller Archeological Museum 586, Jerusalem, Israel.  
lena.brii@gmail.com

**Dr. Valentina Caracuta**

Institute of Evolution Sciences of Montpellier (ISEM). University of Montpellier, CNRS, EPHE, IRD, Montpellier 34090, France.  
valentina.caracuta@umontpellier.fr

**Prof. Amos Frumkin**

Cave Research Center, Fredy and Nadine Herrmann Institute of Earth Sciences, Hebrew University of Jerusalem, Edmond J. Safra Campus — Givat Ram, Jerusalem 9190401, Israel.  
amos.frumkin@mail.huji.ac.il

**Heeli C. Schechter**

Institute of Archaeology, Hebrew University of Jerusalem; Ph.D. honors program of the Jack, Joseph and Morton Mandel School for Advanced Studies in the Humanities, Hebrew University of Jerusalem — Mount Scopus, Jerusalem 9190501, Israel.  
heeli.schechter@mail.huji.ac.il

**Dr. Michael B. Toffolo**

Institut für Naturwissenschaftliche Archäologie, Eberhard Karls Universität Tübingen, Rümelinstraße 23, Tübingen 72070, Germany.  
Institut de Recherche sur les Archéomatériaux-Centre de Recherche en Physique Appliquée à l'Archéologie (IRAMAT-CRP2A), UMR 5060 CNRS, Université Bordeaux Montaigne, 8 Esplanade des Antilles, Pessac 33607, France.  
michael.toffolo@u-bordeaux-montaigne.fr

**Micka Ullman**

Institute of Archaeology, Hebrew University of Jerusalem; Ph.D. honors program of the Jack, Joseph and Morton Mandel School for Advanced Studies in the Humanities, Hebrew University of Jerusalem — Mount Scopus, Jerusalem 9190501, Israel.  
Cave Research Center, Fredy and Nadin Herrmann Institute of Earth Sciences, Hebrew University of Jerusalem, Edmond J. Safra Campus — Givat Ram, Jerusalem 9190401, Israel.  
micka.ullman@mail.huji.ac.il

**Prof. Steve Weiner**

Kimmel Center for Archaeological Science, Scientific Archaeology Unit, Weizmann Institute of Science, 234 Herzl St., Rehovot 7610001, Israel.  
steve.weiner@weizmann.ac.il

**Dr. Lior Weissbrod**

Zinman Institute of Archaeology, University of Haifa, 199 Abba Hushi Avenue, Haifa 3498838, Israel.  
lweissbr@research.haifa.ac.il

**Roni Zuckerman-Cooper**

Zinman Institute of Archaeology, University of Haifa, 199 Abba Hushi Avenue, Haifa 3498838, Israel.  
ronula@gmail.com

## LIST OF FIGURES, TABLES AND PLATES

## Figures

- 1.1.** Topographic map showing the geographical setting of NRQN site
- 1.2.** Aerial photo of the Neshher-Ramla quarry area, black arrow marks the location of NRQN site (looking northwest)
- 1.3.** Plan of NRQN site, showing the excavation grid layout and location of sections
- 1.4.** Section C–C' (east–west) showing the sinkhole contours and the damage caused by the backhoe to the upper part of the site (marked by diagonal hatching)
- 1.5.** Map showing archaeological sites mentioned in this volume. (a) The southwestern Levant; (b) The Levant. Modern cities are marked by rectangles
- 1.6.** The pedogenic limestone calcrete crust cover (*nari*) in the area of NRQN sinkhole, after soil stripping (looking northeast)
- 2.1.** Location, geology and topography of the study area (modified after Frumkin et al. 2015). (a) Geological map of the Neshher-Ramla quarry and its recharge zone in the Ramallah Anticline. Thin black lines are faults; (b) Schematic geological section along the line shown in (a), crossing the central mountain ridge. Possible flow routes of artesian water are shown by arrows. Albian marls serve as an aquiclude at the base of the Yarkon-Taninim Aquifer. Albian-Turonian carbonates with interbedded marl layers carry the aquifer. Cenomanian-Turonian marls and Senonian chalk partly confine the aquifer. Impervious Cretaceous to Quaternary sediments of the Coastal Plain block the western side of the aquifer; (c) Topographic map
- 2.2.** Rock and soil cover at the NRQN sinkhole vicinity: bottom — Menuha Formation Senonian chalk; center — pedogenic calcrete — *nari* (caliche) limestone; top — dark clay soil
- 2.3.** Section A–A' (north-south) vertical section through the NRQN sinkhole, with the location of radiocarbon samples and date range (cal BP range of 95% probability, after Toffolo and Boaretto, Chapter 4)
- 2.4.** The geometry of NRQN sinkhole, presented by vertical (left) and horizontal (right) sections.
- 2.5.** View of the NRQN sinkhole section from the southwest. Note whitish chalk fragments and dark clay fill between the chalk walls
- 2.6.** Tilted sediments in the northern part of the NRQN sinkhole
- 2.7.** A sinkhole filled with geogenic gravels embedded in clay, with partially overhanging *nari*, ~10 m north of the NRQN sinkhole, and similar in size
- 3.1.** Section A–A' (north–south), showing vertical division of the site stratigraphy into three units (1–3) (blue lines), and the main man-made features (red lines)
- 3.2.** Section A–A' (north–south) showing loci position
- 3.3.** Section B–B' (north–south) showing loci positions. Diagonal hatches mark the part of the sinkhole that was dug out and damaged by the backhoe
- 3.4a.** Plan of the site at elevation 102.40–45 m asl
- 3.4b.** Plan of the site at elevation 101.0–85 m asl
- 3.4c.** Plan of the site at elevation 100.70–90 m asl
- 3.4d.** Plan of the site at elevation 100.05–15 m asl, showing the location of the complete aurochs rib
- 3.4e.** Plan of the site at elevation 99.80–90 m asl, showing the location of the partial human skull
- 3.5.** Photo of sediments accumulation within the sinkhole, along section A–A' (looking east): (a) Units 1 and 2; (b) Units 2 and 3

- 3.6. Photo of Hearth L.15S65–0010, overview
- 3.7. Photo of Hearth L.15S65–0010, section view (looking northeast)
- 3.8. Photo of the stratified sediments of Unit 2, tilting toward the center of the sinkhole: looking south (left), looking north (right)
- 3.9. Photo of Stone Cluster L.15S65–0038, overview
- 3.10. Photo of the three hewn footholds in the northern wall of the sinkhole (looking north)
- 4.1. Bayesian model incorporating the four high-quality dates of NRQN. Boundaries are set according to the site stratigraphy (Units 1, 2 and 3)
- 4.2. Probability distributions of radiocarbon dates. The NRQN dates appear in a dark gray shade and are shown in stratigraphic order from top to bottom. Probability distributions shown in red are the earliest and latest dates obtained from the EPPNB site of Motza (Yizhaq et al. 2005)
- 5.1. Helwan projectile points. (a) Item F021; (b) Item F022; (c) Item F018
- 5.2. Tools made of high-quality exotic flint. (a) Borer with reddish (heated?) tip, item F017; (b) Burin on reaping knife, item F028; (c) Reaping knife, item F020
- 5.3. Bifacial tools made of local brecciated Mishash flint
- 5.4. Hammerstones
- 5.5. Flint tools made of local flint
- 5.6. Flint tools made on bi-directional blade blanks and high-quality exotic flint
- 6.1. River-pebble accumulation in the streambed of Nahal Ayyalon
- 6.2. Fragment of stone bowl rim coated with ochre
- 6.3. Stone bowl fragments, note the numerous striation signs on their surface
- 6.4. Pestles
- 6.5. Perforated objects
- 7.1. Bi-conical pendant made of chalk
- 7.2. Engraved limestone object
- 7.3. Pumice object
- 7.4. Geometric baked clay object
- 8.1. A 3D model of the human skull fragment
- 8.2. The human skull fragment *in situ* during excavation
- 8.3. The human skull fragment. (a) Note the thick supra-orbital ridges (thin arrow) and the pronounced glabella (dashed arrow); (b) Note the sloping forehead from the lateral view (thin arrow); (c) A depressed fissure evident above the left supra-orbital ridge, about 20 mm long, oblique and smooth on one side (thin arrow) and jagged on the other side (dashed arrow)
- 9.1. Fusion information for aurochs (n=21). The fusion of the bone elements by months: 0-proximal metapodial; 7–18–1st, 2nd and 3rd phalanges; 24–30 — distal metacarpal and distal metapodial; 36–42 — calcaneum; 42–48 — proximal femur, proximal humerus and distal radius. For detailed fusion information of each bone element, see Appendix 9.II.
- 9.2. Cut marks on a bone (no. 267; L.15S65–0003)
- 9.3. Worked bone fragments: burnt with striations on the shaft surface (nos. 194 and 195; L.15S65–0003)
- 9.4. Body-part distribution of large (based on MNE=40) and medium ungulates (based on MNE=52) in NRQN assemblage
- 9.5. Frequency of the main taxa in faunal assemblages from EPPNB and MPPNB sites
- 9.6. The complete aurochs rib *in-situ*, during the excavation of Unit 3 (L.16S65–3007; B.16S65–30183)
- 10.1. Section A-A' (north-south) of the NRQN sinkhole, indicating loci with high microvertebrate NISPs (>50; light gray shading). The division between stratigraphic units is marked by a blue line
- 10.2. Boxplot distribution of NISPs of all analyzed loci (n=49) in Squares M6–8 in the NRQN sinkhole

- 10.3.** Frequencies of skeletal elements of small mammals, based on the equation: NISP per element / MNI × number of times that each element occurs in a complete skeleton (Andrews 1990: 45). The minimum number of individuals per assemblage is obtained from the range of values of element NISPs where for each element, its NISP is divided by the number of times that the element occurs in a complete skeleton. The largest value in this range is then used as the assemblage MNI
- 10.4.** Frequencies of skeletal elements of amphibians
- 11.1.** Shells from NRQN. (a) *Mauritia grayana*; (b) *Neverita josephinia*; (c, d) *Columbella rustica*; (e) *Tritia gibbosula*; (f, g) *Conus ventricosus*; (h, i) *Pirenella conica*; (j) *Cerithium vulgatum*; (k) *Hexaplex trunculus*; (l) *Antalis rossati*; (m) *Antalis dentalis*; (n-q) *Glycymeris nummaria*; (r) *Acanthocardia tuberculata*; (s) *Donax trunculus*.
- 11.2.** Perforated *Columbella rustica* shells. (a) Parallel oblique abrasion striations around perforation; (b, c) Irregular perforation circumference; (d) Indentations on shell base
- 11.3.** *Conus ventricosus* shells. (a) Abraded plain oblique to shell axis — 98°; (b) Abraded plain oblique to shell axis — 87°; (c, d) Striations on unburnt *Conus*; (e) Ocher stain in perforation; (f) Ocher stain in base of aperture; (g, h) Slight chipping and asymmetry in perforation circumference; (i, j) Chipping on aperture base; (k, l) Flattening by abrasion of aperture base
- 11.4.** A *Nerita sanguinolenta* shell. (a) Location of perforation; (b) Flattening of perforated area; (c) Irregular perforation circumference; (d) Indentation in perforation circumference
- 11.5.** A *Mauritia grayana* shell. (a) Polished dorsum break on inner lip; (b) Polished columella break on inner lip; (c) Striations on outer lip
- 11.6.** *Pirenella conica* shells. (a, b) Single perforation; (c) Two perforations; (d) Remnants of the smoothed circumference of a broken perforation; (e, f) Effects of stringing — indentations and smoothing of notches on broken apertures, in relation to perforations
- 11.7.** A *Tritia gibbosulus* shell. (a) Notches on left side of perforation circumference; (b) Notches on right side of perforation circumference; (c) Several plains of abrasion; (d) Highly abraded and smoothed base break
- 11.8.** A *Theodoxus jordani* shell. (a) Perforation; (b) Indentation on aperture; (c) Indentation on perforation circumference; (d) Striations on body whorl; (e) Striations on inner lip
- 12.1.** The location of NRQN site and PPNB sites mentioned in the text. Modern cities are marked by rectangles
- 12.2.** Photo of the charred seeds retrieved from NRQN site. (a) Ventral and lateral view of *Vicia faba* sp.; (b) Ventral and lateral view of *Lathyrus hirosolymitanus*; (c) Lateral view of *Lens* sp. Photos were taken with Leica DFC295 connected to a Leica M80 stereomicroscope
- 12.3.** The distribution of the faba bean in the northern and southern Levant during the Pre-Pottery Neolithic. Modern cities are marked by rectangles
- 13.1.** Composite picture showing section A-A' (north-south) of the sinkhole and the archaeological layers identified during the excavation (divided by dashed lines). The arrow indicates where the orange sediment abuts a pile of limestone cobbles
- 13.2.** Composite picture showing section A-A' (north-south) of the sinkhole and the location of bulk, block and radiocarbon dating samples, and relative FTIR and  $\mu$ FTIR results. Black lines mark the dark lenses rich in ash and charcoal. The white solid line delimits the orange clay layer
- 13.3.** FTIR spectra of control and archaeological samples heated to different temperatures and their admixtures (a.u.:

- arbitrary units). The absorption band at  $1433\text{ cm}^{-1}$  belongs to calcite, whereas the bands at  $797$ ,  $779$ ,  $694$ ,  $516$  and  $466\text{ cm}^{-1}$  belong to quartz. Other absorptions are explained in the text
- 13.4.** Plot showing the characteristic trendlines of standard calcite materials with different degrees of atomic order (modified after Regev et al. 2010), and data points for control and archaeological samples from NRQN (n.a.u.: normalized absorbance units)
- 13.5.** Photomicrographs of thin sections. (a) Clusters of rhomb-shaped ash pseudomorphs (arrows) embedded in a charcoal fragment from the dark lens of Block 2, plane polarized light (PPL); (b) Phytolith-rich groundmass (PPL, Block 2). The arrow indicates a phytolith multicell composed of leaf/stem morphotypes; (c) Fragment of burnt limestone from the dark lens, showing shrinkage cracks, carbonation fronts and sparitic crystals of calcite (PPL, Block 2); (d) Rounded pellet of burnt silty clay (PPL, Block 4); (e) Aggregate of melted silica, quartz and clay (PPL, Block 1). Note the bubbles left by the escape of water upon burning; (f) Fragment of lime plaster-like material rich in quartz silt, showing voids caused by the inclusion of plant material (arrows; PPL, Block 5); (g) Fragment of lime-plaster-like material rich in quartz silt (PPL, Block 6); (h) Same as (g), in crossed-polarized light. Circles mark sand-sized lime lumps; note the banded carbonation fronts
- 13.6.** Scan of a thin section from Block 2, showing the dark lens (between dashed lines) embedded in brown clay, and  $\mu\text{FTIR}$  spectra of representative components (short side of frame: 5 cm). (a, b) show reflectance spectra of burnt limestone fragments characterized by the absorption band of lime plaster calcite at  $1415\text{--}1410\text{ cm}^{-1}$
- 13.7.** Scan of a thin section from Block 1, showing the transition between the porous ash layer of the dark lens (between dashed lines) and the reddened sediment beneath it, and  $\mu\text{FTIR}$  spectra of representative components (short side of frame: 5 cm). (a) Reflectance spectrum of burnt limestone fragment showing the absorption band of lime plaster calcite at  $1415\text{--}1410\text{ cm}^{-1}$ ; (b) Transmission spectrum of burnt silty clay pellet, characterized by the absence of clay minerals absorptions in the  $3700\text{--}3600\text{ cm}^{-1}$  region
- 13.8.** Scan of a thin section from Block 4, showing the brown clay (top), the dark lens (middle) and the orange clay (bottom), and  $\mu\text{FTIR}$  spectra of representative components (short side of frame: 5 cm). (a) Reflectance spectrum of unheated limestone fragment showing the absorption bands of micritic limestone at  $1480$  and  $1410\text{ cm}^{-1}$ ; (b) Transmission spectrum of burnt silty clay pellet, characterized by the absence of clay minerals absorptions in the  $3700\text{--}3600\text{ cm}^{-1}$  region
- 13.9.** Scan of a thin section from Block 6, showing the transitions between the dark lens (middle) and the orange clay above and below it, and  $\mu\text{FTIR}$  spectra of representative components (short side of frame: 5 cm). (a) Reflectance spectrum of burnt limestone fragment showing the absorption band of lime plaster calcite at  $1415\text{--}1410\text{ cm}^{-1}$ ; (b) Transmission spectrum of burnt silty clay pellet, showing weak absorption bands of clay minerals at  $3697$  and  $3621\text{ cm}^{-1}$ , consistent with low-temperature burning ( $< 500\text{ }^{\circ}\text{C}$ )
- 14.1** Section A-A' of NRQN sinkhole (north-south), showing the division into three stratigraphic units (separated from one another by blue lines); manmade features (red lines); microvertebrate bone concentrations (gray shading); and vertical distribution of groundstone tools, flint tools and shells. Only items with secure locations were plotted
- 14.2.** EPPNB sites in the southwestern Levant: Horvat Galil (Gopher 1997), Ahihud (Caracuta et al. 2017), Mujahiya (Gopher



1990), Kh. 'Asafna East (van den Brink 2017), Kfar HaHoresh (Birkenfeld 2018), Mishmar Ha'Emeq (Barzilai et al. 2011), Tel 'Ali (Prausnitz 1966), el-Wad, Sefunim and Kebara caves (Belfer-Cohen and Goring-Morris 2007), Nahal Oren (Noy, Legge and Higgs 1973; Barzilai 2009), Michmoret 26 and 26A (Burian and Friedman 1965), Jericho (Crowfoot-Payne 1983; Gopher 1994), Motza (Yizhaq et al. 2005), Qumran Cave 24 (Gopher

et al. 2013: Table 1), Nahal Lavan 109 (Burian, Friedman and Mintz 1976, 1999), Nahal Boqer (Noy and Cohen 1974) and Abu Salem (Gopher and Goring-Morris 1998)

- 14.3.** Proposed reconstruction of the sinkhole in use as a semi-subterranean hut. If the sinkhole was partially capped by a *nari* overhang, in which case the manmade roofing may have been smaller

### List of Tables

- |                                                                                                                                                                                                                                                                                                                                                                                                                                                                                                                                                                                                                                                                                                                                                                                                                                                                                                                                                                                                                                                                                                                                                                                                                                                                                                                                                                             |                                                                                                                                                                                                                                                                                                                                                                                                                                                                                                                                                                                                                                                                                                                                                                                                                                                                                                                                                                                                                                                                                                                                                                                                                                                                                                                                                                                                |
|-----------------------------------------------------------------------------------------------------------------------------------------------------------------------------------------------------------------------------------------------------------------------------------------------------------------------------------------------------------------------------------------------------------------------------------------------------------------------------------------------------------------------------------------------------------------------------------------------------------------------------------------------------------------------------------------------------------------------------------------------------------------------------------------------------------------------------------------------------------------------------------------------------------------------------------------------------------------------------------------------------------------------------------------------------------------------------------------------------------------------------------------------------------------------------------------------------------------------------------------------------------------------------------------------------------------------------------------------------------------------------|------------------------------------------------------------------------------------------------------------------------------------------------------------------------------------------------------------------------------------------------------------------------------------------------------------------------------------------------------------------------------------------------------------------------------------------------------------------------------------------------------------------------------------------------------------------------------------------------------------------------------------------------------------------------------------------------------------------------------------------------------------------------------------------------------------------------------------------------------------------------------------------------------------------------------------------------------------------------------------------------------------------------------------------------------------------------------------------------------------------------------------------------------------------------------------------------------------------------------------------------------------------------------------------------------------------------------------------------------------------------------------------------|
| <p><b>3.1.</b> Description of Units 1, 2 and 3, top and bottom elevations and related loci</p> <p><b>4.1.</b> Radiocarbon dates of NRQN (high-quality samples are in bold) and the earliest and latest radiocarbon dates from EPPNB Motza (Yizhaq et al. 2005)</p> <p><b>5.1.</b> General breakdown of the flint assemblage</p> <p><b>5.2.</b> Raw material type according to tool type</p> <p><b>5.3.</b> Core frequencies by targeted blank</p> <p><b>5.4.</b> Frequency of tool blanks</p> <p><b>5.5.</b> Core type frequencies</p> <p><b>5.6.</b> Tool preservation conditions complete/broken, by tool type</p> <p><b>5.7.</b> Tool preservation conditions burnt/unburnt, by tool type</p> <p><b>5.8.</b> Projectile points</p> <p><b>5.9.</b> Breakdown of perforators by sub-type</p> <p><b>5.10.</b> Tool type frequencies at PPNB sites in the Mediterranean climate zone of the southern Levant</p> <p><b>5.11.</b> Component frequencies of chipped flint assemblages from PPNB sites in the Mediterranean climate zone of Israel</p> <p><b>5.12.</b> Perforators frequency at PPNB sites</p> <p><b>6.1.</b> General breakdown of groundstone tool types</p> <p><b>6.2.</b> Breakdown of groundstone tools by raw materials</p> <p><b>6.3.</b> Distribution of groundstone tool types by blanks</p> <p><b>6.4.</b> Groundstone tools preservation breakdown</p> | <p><b>6.5.</b> Vessel sub-types</p> <p><b>6.6.</b> General breakdown of the flaked limestone industry</p> <p><b>6.7.</b> Limestone wedges</p> <p><b>9.1.</b> Fauna species breakdown by unit in the NRQN assemblage</p> <p><b>9.2.</b> Fusion data for mountain gazelle (n=14)</p> <p><b>9.3.</b> Taphonomic data for the NRQN faunal assemblage</p> <p><b>9.Ia.</b> Counts of anatomical elements (NISP and MNE) for each specimen</p> <p><b>9.Ib.</b> Counts of anatomical elements (NISP and MNE) for each specimen</p> <p><b>9.II.</b> Detailed fusion information by each bone element, for <i>Bos primegenius</i> and <i>Gazella gazella</i></p> <p><b>9.III.</b> Animal representation in EPPNB and MPPNB sites: NRQN (current study), Motza (Khalaily et al. 2007), Abu Ghosh (Kolska Horwitz 2003), Kfar HaHoresh (Meier et al. 2016) and Yiftahel (Alhaique and Kolska Horwitz 2012; Sapir-Hen et al. 2016)</p> <p><b>9.IV.</b> Anatomical measurements (mm) of the NRQN assemblage</p> <p><b>10.1.</b> Numbers of identified specimens (NISP) by taxa, excavation squares and loci. Loci marked by hatched lines belong to the middle unit, separating the upper from the lower units (see also Fig. 10.1). Brown shading indicates loci with &gt;50 NISP and gray shading loci with &gt;100 NISP</p> <p><b>10.2.</b> Comparative table of contextual, taxonomic and taphonomic</p> |
|-----------------------------------------------------------------------------------------------------------------------------------------------------------------------------------------------------------------------------------------------------------------------------------------------------------------------------------------------------------------------------------------------------------------------------------------------------------------------------------------------------------------------------------------------------------------------------------------------------------------------------------------------------------------------------------------------------------------------------------------------------------------------------------------------------------------------------------------------------------------------------------------------------------------------------------------------------------------------------------------------------------------------------------------------------------------------------------------------------------------------------------------------------------------------------------------------------------------------------------------------------------------------------------------------------------------------------------------------------------------------------|------------------------------------------------------------------------------------------------------------------------------------------------------------------------------------------------------------------------------------------------------------------------------------------------------------------------------------------------------------------------------------------------------------------------------------------------------------------------------------------------------------------------------------------------------------------------------------------------------------------------------------------------------------------------------------------------------------------------------------------------------------------------------------------------------------------------------------------------------------------------------------------------------------------------------------------------------------------------------------------------------------------------------------------------------------------------------------------------------------------------------------------------------------------------------------------------------------------------------------------------------------------------------------------------------------------------------------------------------------------------------------------------|

- characteristics of pitfall assemblages of microvertebrate species, contrasting the NRQN assemblage (gray shading) with documented examples from different periods in the U.S. and U.K.
- 10.3.** Relative frequencies (%) of microvertebrate classes in the NRQN assemblage, compared with three other regional Pleistocene-period sites
- 10.4.** Indices of species diversity of small mammals in the NRQN assemblage, compared to three other regional Pleistocene-period sites. The majority of indices show that diversity is highest and taxonomic dominance (Dominance\_D and Berger-Parker) lowest in the NRQN assemblage, indicated by shaded cells
- 11.1.** Marine shell taxa from NRQN
- 11.2.** Freshwater shells from NRQN — each row represents a single specimen
- 11.3.** Marine shells — distribution by class
- 11.4.** Marine shells — distribution by origin
- 11.5.** Marine shells — naturally perforated
- 11.6.** Marine shells — appearance of each taxon within the heated assemblage, and of heated items within each taxon
- 11.7.** Marine shells — comparison of the frequencies of various heated items
- 11.8.** Marine shells — artificially perforated or otherwise worked shells. Most of the worked specimens (NISP in the left column) have more than one type of working
- 11.9.** Marine shell counts from PPNB sites in the Mediterranean zone of Israel
- 12.1.** Wood charcoals identified at NRQN
- 12.2.** Seeds identified at the NRQN site
- 13.1.** Microfacies types (MFT) identified at NRQN

### List of Plates

- 5.1.** Chipped flint assemblage: debitage and core trimming elements (CTEs)
- 5.2.** Chipped flint assemblage: spalls
- 5.3.** Chipped flint assemblage: cores
- 5.4.** Chipped flint assemblage: cores
- 5.5.** Chipped flint assemblage: projectile points
- 5.6.** Chipped flint assemblage: perforators
- 5.7.** Chipped flint assemblage: perforators
- 5.8.** Chipped flint assemblage: sickle blades
- 5.9.** Chipped flint assemblage: retouched blades
- 5.10.** Chipped flint assemblage: microlith and scrapers
- 5.11.** Chipped flint assemblage: burins and notches
- 5.12.** Chipped flint assemblage: multiple tools
- 5.13.** Chipped flint assemblage: bifaces
- 5.14.** Chipped flint assemblage: various tools
- 5.15.** Hammerstones
- 6.1.** Groundstone tools: lower grinding tool
- 6.2.** Groundstone tools: handstones
- 6.3.** Groundstone tools: handstones
- 6.4.** Groundstone tools: handstones
- 6.5.** Groundstone tools: massive handstones
- 6.6.** Groundstone tools: massive handstones
- 6.7.** Groundstone tools: mortars
- 6.8.** Groundstone tools: bowlets
- 6.9.** Groundstone tools: bowls
- 6.10.** Groundstone tools: pestles
- 6.11.** Groundstone tools: pestles
- 6.12.** Groundstone tools: perforated objects
- 6.13.** Groundstone tools: pick-like tools
- 6.14.** Groundstone tools: choppers
- 6.15.** Groundstone tools: bifacial-disk-like tools
- 6.16.** Groundstone tools: pallets
- 6.17.** Groundstone tools: limestone slab
- 6.18.** Groundstone tools: others
- 6.19.** Limestone industry: primary flakes and flakes
- 6.20.** Limestone industry: twisted spall, other and wedges

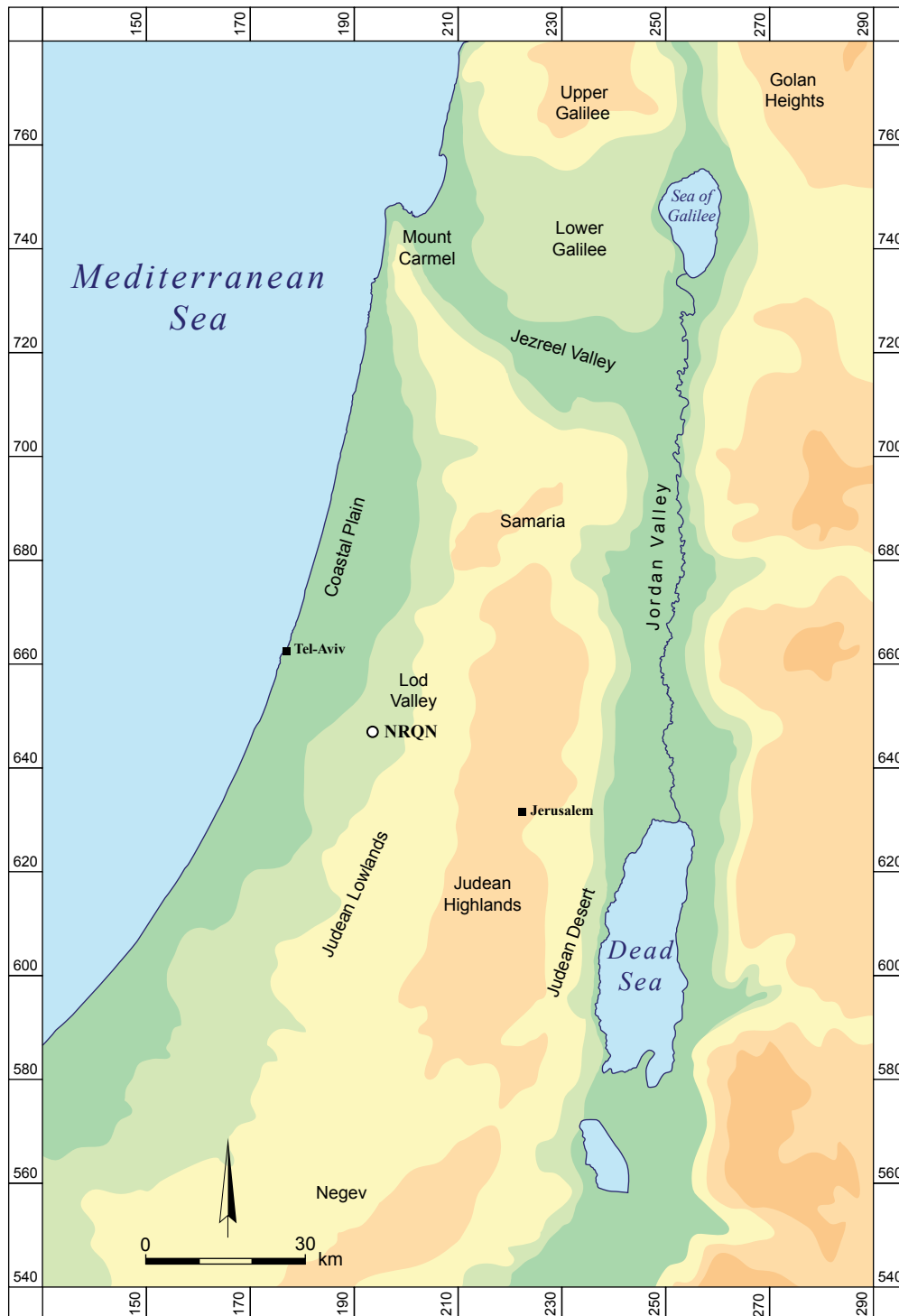


**Fig. 1.1.** Topographic map showing the geographical setting of NRQN site